JOURNAL OF SPACECRAFT AND ROCKETS
Vol. 33, No. 6, November–December 1996

# Computational and Experimental Investigations of Ionization near Hypersonic Vehicles

V. A. Gorelov,* M. K. Gladyshev,† A. Y. Kireev,† A. S. Korolev,† and I. V. Yegorov†
*Central Aerohydrodynamic Institute, Zhukovsky-3, Moscow Region 140160, Russia*
and
V. N. Byzov‡
*Flight Research Institute, Zhukovsky-3, Moscow Region 140160, Russia*

**Investigations of ionization processes near hypersonic vehicles are reviewed. The investigations include the numerical simulation of ionization in nonequilibrium viscous shock layers; an experiment on ionization measurement during flight tests, which were carried out using Russian vehicles Bor-4c; and model investigations in a high-enthalpy hot-shot-type wind tunnel. Particular emphasis was placed on the wind-tunnel tests by applying the approximate method of ionization simulation in flows with viscous shock layers. Some examples showing the possibilities of ionization investigation near vehicles and their components are given.**

## Nomenclature

$H$ = flight altitude
$k$ = reaction rate constant
$M$ = Mach number
$n$ = concentration
$P$ = pressure
$R$ = nose radius
$Re_0$ = Reynolds number, $(\rho_\infty V_\infty R)/\mu_0$
$S$ = coordinate along the surface of body
$Sc_i$ = Schmidt number
$T$ = temperature
$t$ = flow time
$u$ = flow velocity
$V$ = flight velocity or freestream velocity in the wind tunnel
$X$ = coordinate along the vehicle axis
$Y$ = coordinate normal to axis of the vehicle
$Y_V$ = coordinate normal to velocity $V_\infty^*$
$y$ = coordinate normal to the body
$\alpha$ = angle of attack
$\Lambda$ = correlation parameter, $\Lambda = t/\tau$
$\mu$ = viscosity of gas
$\rho$ = density
$\tau$ = characteristic time of process

*Subscripts*

$d$ = dissociation
$e$ = electron
$i$ = ion, ionization
$k$ = $k$th species
$m$ = maximum value
qs = quasistationary
$r$ = recombination
$s$ = conditions behind the shock wave
$v$ = vibration
$w$ = wall conditions
0 = stagnation value
$\infty$ = freestream

*Superscripts*

eq = equilibrium
$*$ = test conditions

Presented as Paper 95-1940 at the AIAA 26th Plasmadynamics and Lasers Conference, San Diego, CA, June 19–22, 1995; received June 28, 1995; revision received March 15, 1996; accepted for publication June 15, 1996. 

*Deputy Head, Hypersonic Department, and Head, Aerophysical Division.
†Leading Scientist, Aerophysical Division.
‡Deputy Head of Department.

## Introduction

THIS paper presents a review of investigations carried out at the Central Aerohydrodynamic Institute (TsAGI) and at the Flight Research Institute to evaluate the gas ionization peculiarities during atmospheric flights at velocities up to 8 km/s. Most of the investigations were accomplished in the 1980s when the problems of communication through plasma formations were solved for vehicles of different purposes. Some important results have been obtained in recent years.

Gas ionization near vehicles flying in the atmosphere at velocities of 4–8 km/s is a complicated process requiring the consideration of various factors, depending on flight conditions. Ionization of easily ionized impurities entering the boundary layer as a result of thermal decomposition of thermal protection materials is of great importance in flights at altitudes lower than 60 km. This effect is beyond the scope of the present paper; all attention is concentrated on air ionization processes in flights at altitudes above 60 km at conditions under which ionization of those impurities can be neglected. In this case, the primary focus is on the nonequilibrium nature of ionization in a viscous shock layer and factors influencing this process.

We apply a complex approach to the investigation of ionization effects, including numerical simulation, a laboratory model experiment, and a flight experiment. All constituents of this triad are presented, but particular attention is paid to the simulation of approximately nonequilibrium ionization processes in high-enthalpy wind tunnels.

## Hypersonic Flight Envelope Under Study

To characterize the nonequilibrium level of ionization in flows over bodies, the parameter $\Lambda = t/\tau$ can be introduced, where $t$ is the characteristic time of gas particle motion through a region under study and $\tau$ is the time characterizing ionization or recombination processes. For the ionization process in a shock layer near the stagnation point of a blunted body, we have $\Lambda_i \approx R/(V_\infty \tau_i)$, where $R$ is the radius of nose bluntness and $\tau_i$ is the characteristic time of gas ionization behind the normal shock wave.[1] Note that $\Lambda_i \approx 0.8\,[(R/V_\infty \tau_i)]\,\ell n(\delta/\Delta)$ ($\delta$ is the boundary layer thickness) for a nonequilibrium inviscid shock layer when the gas velocity behind the shock wave is $u \approx (\rho_\infty/\rho_s)V_\infty(y/\Delta)$ [$\Delta \approx 0.8(\rho_\infty/\rho_s)R$ is the shock-wave standoff distance]. As for a viscous shock layer, the linear dependence of $u$ on $y$ is not exhibited, and the relation for $\Lambda_i$, outlined above, is only of a qualitative nature. Direct

computations can show that, at $\Lambda_i \geq 1$, a maximum ionization level behind the shock wave is close to equilibrium. The parameter $\Lambda_r = t/\tau_r$ can be introduced for flow regions, where recombination processes are of first importance. It was established that in considering a gas flow over spherical bluntness, when only one governing reaction of binary recombination is taken into account (e.g., $NO^+ + e \rightarrow N + O$), the relaxation similarity parameter can be expressed as $\Lambda_r \approx (k_{r0} n_{e0} R)/V_\infty$, where $k_{r0}$ is the recombination rate constant at the stagnation point. From the parametric computations, it can be inferred that ionization close to equilibrium takes place in the recombination zones at $\bar{S}_0 = S_0/R \leq 1.5$, when $\Lambda_r > 10^3$, whereas the regime with "frozen" ionization is observed at $\Lambda_r \leq 2$. The extent to which dissipative processes affect the quantity $n_e$ in the shock layer can be estimated using $Re_0 = \rho_\infty V_\infty R/\mu_0$, where $\mu_0$ is viscosity determined at the stagnation temperature behind the shock wave. The computations reveal that, in the viscous shock layer regime, the dissipative processes influence the maximum electron concentration $n_{e0,m}$ at $Re_0 \leq 10^2$. Figure 1 presents, in the $H$-$V$ coordinates, the characteristic regimes of ionization conditions in a hypersonic flight. Bands 1 and 2 correspond to $\Lambda_r = 10^3$ and 2, respectively; band 3 corresponds to $\Lambda_i = 1$; and band 4 corresponds to $Re_0 = 100$. Upper and lower boundaries of these regions correspond to $R = 1.0$ and 0.1 m, respectively. When the velocity and altitude of vehicle flight correspond to the region lying below band 1, the ionization processes near the side surface of the vehicle are close to equilibrium. In the region between bands 1 and 2, the recombination processes are substantially nonequilibrium, and above band 2, the recombination can be assumed to be frozen. In the region above band 3, the equilibrium level of ionization is not attained in the vicinity of the stagnation point, and in the area above band 4, the flow condition is typical for a viscous shock layer and the $n_e$ level is essentially influenced by dissipative processes. Curve 5 in Fig. 1 illustrates the flight trajectory for the Bor-4c vehicle.

Now, we define briefly the limitations resulting from the peculiarities of the statement of the problem and the methods of its solution. Neglecting the influence of easily ionized impurities entering the gas attributable to the thermal decomposition of thermal protection materials used in hypersonic vehicles restricts the altitude under study to $H > 60$ km. Special features of experimental methods applied to investigate ionization further restrict the flight altitude. In flight experiments, the ion concentration inside the shock layer was measured by using fixed cylindrical probes, which were destroyed at $H < 70$ km. The upper limit of the probe applicability is set by the altitude of $H < 105$ km because of the difficulties encountered in onboard measurements of probe current in a very wide (about 5 orders of magnitude) range of its variation. In laboratory conditions, the altitude range for the simulation of ionization depends on both the technical factors (limits in enthalpy and wind-tunnel start conditions) and the capabilities of approximate simulation of nonequilibrium ionization (see later). For the numerical simulation, the flight-altitude limit was restricted by the continuum model to about 100 km for a vehicle with $R \approx 1$ m. Thus, the scope of complex investigations of properties inherent in the ionization process when a hypersonic vehicle re-enters at $V \approx 7$–$8$ km/s was bounded in the present study by a lower altitude of approximately 75 km and an upper altitude of 105 km. As shown in Fig. 1, the regime of nonequilibrium ionization in a viscous shock layer is realized near the vehicle bluntness when nonequilibrium or frozen recombination processes proceed in the zones of expanded concurrent flows. The features of ionization processes taking place under these conditions were taken into account in the numerical and experimental investigations.

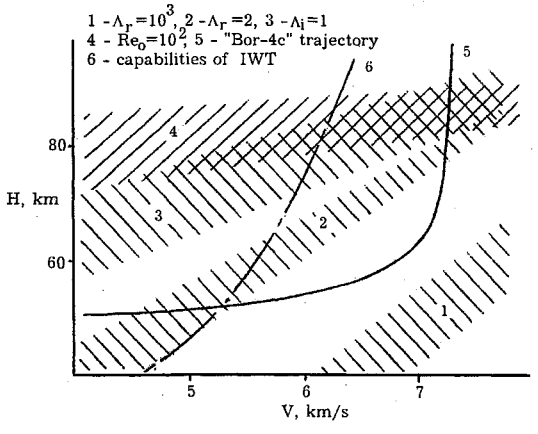


**Fig. 1 Characteristic regimes of ionization conditions in hypersonic flight.**

## Numerical Simulation

The numerical model employed to determine the ionization level at the flight conditions under study must consider a high level of nonequilibrium of physical–chemical processes in a viscous shock layer, the influence of dissipative processes, and surface boundary conditions. The two-dimensional model using full Navier–Stokes equations (NS model) was our main numerical tool, but its use was dependent on available computer resources. However, in most cases, the use of wind-tunnel test data on flows over bodies of simple configuration was sufficient to determine the ionization levels relative to real vehicles. Consideration was given to an air model comprising $O_2$, $N_2$, NO, O, N, $NO^+$, $O_2^+$, $N_2^+$, $e^-$. The kinetic model of nonequilibrium processes in the viscous shock layer involved the nonequilibrium vibrational excitation of $N_2$, $O_2$, and NO; the dissociation of $N_2$, $O_2$, and NO; the associative ionization reactions resulting in $NO^+$, $N_2^+$, and $O_2^+$; and the exchange reactions with participation of neutral atoms, molecules, and ions. The reaction rate constants were taken from other research.[2,3] The rotational temperature $T_r$ was assumed to be equal to the translational temperature $T$. The influence of vibration relaxations on dissociation reactions was taken into account by two-temperature dependence of the reaction rate constant in accordance with the model of effective vibrational level ($\beta$ model of dissociation).[3] Accordingly, the dissociation rate was determined as

$$k_d(T, T_{v,k}) = k_d(T)\Phi(T, T_{v,k}) \tag{1}$$

where

$$\Phi(T, T_{v,k}) = \frac{1 - \exp(-\theta_k/T_{v,k})}{1 - \exp(-\theta_k/T)} \exp\left[-(D_k - \beta_k T)\left(\frac{1}{T_{v,k}} - \frac{1}{T}\right)\right]$$

and $\theta_k$ is the characteristic vibrational temperature of the $k$th species and $D_k$ is the dissociation energy (in degrees Kelvin).

The values $\beta_k$ were assumed to be constant (1.5 for $O_2$ and 3.0 for $N_2$ and NO). The one-temperature rate constants $k_d(T)$ for dissociation reactions were taken from Losev et al.[3] The interaction between vibrational and translational degrees of freedom ($V$-$T$ exchange) was simulated by using the Landau–Teller equations. The vibrational relaxation times were determined on the basis of the data of Losev et al.[3] The $V$-$V$ exchange for molecular species $k$ and $j \neq k$ was simulated by application of the expression

$$Q_{vv,k} = \rho^2 N_A C_k \frac{\theta_k R_U}{M_k} \sum_{\substack{j=1 \\ j \neq k}}^{K} X_j F_{j,k}(T)$$

$$\times \left[e_{v,j}(1 + e_{v,k}) - e_{v,k}(1 + e_{v,j}) \exp \frac{(T_{v,k} - T_{v,j})}{T}\right] \tag{2}$$

where

$$e_{v,k} = \frac{1}{\exp(\theta_k/T_{v,k}) - 1}$$

$N_A$ is Avogadro's number, $R_U$ is the universal gas constant, $M$ is the molecular weight, $C$ is the specie mass fraction, and $X_j = C_j/M_j$ is the molar concentration of $j$ species. The function $F_{j,k}(T)$ was determined on the basis of other data.[4]

The variation in vibrational energy of molecular specie $k$ attributable to chemical reactions $Q_{vc,k}$ was calculated by employing the relation

$$Q_{vc,k} = M_k \left[\sum_{l=1}^{L} r_{k,l} \frac{(D_k - \beta_k T) R_U}{M_k} + \sum_{l=L+1}^{L+2} r_{k,l} e_{v,k}\right] \tag{3}$$

where $r_{k,l}$ is the reaction rate, $L = 15$ is the quantity of dissociation reactions, and $l$ is the number of reactions. In relation (3), the first term answers for dissociation reactions. It is supposed that average variations of species vibrational energy at the unit dissociation and recombination are equal to $(D_k - \beta_k T)R_U/M_k$. The second term in Eq. (3) describes the exchange reactions, and the mean variation in the specific vibrational energy for each step of the exchange reaction is equal to the specific vibrational energy of a newly forming or disappearing molecule.

At the surface, no-slip boundary conditions as well as boundary conditions for heterogeneous recombination reactions and heat balance were considered. It was assumed that $C_{kw} = 0$ for atoms and ions on an ideally catalytic surface and $(dC_k/dy)|_w = 0$ on a noncatalytic surface. The combined boundary conditions also were considered, e.g., $C_{Ow} = 0$, $C_{Nw} = 0$; $(dC_{NO}/dy)|_w = 0$. The generalized Rankine–Hugoniot conditions were given on the shock wave. The transfer coefficients were calculated by use of empirical formulas of Wilke and Mason–Saxena, based on the potential of Lenard–Jones. For the calculation of heat conductivities of molecular components, the correction of Euken was introduced. The diffusion factors were determined from the condition of constant Schmidt numbers $Sc_i$, which were assumed to be equal to 0.5 for neutral components of the gas mixture and 0.25 for ions, the self-diffusion coefficients being calculated by applying the condition $Sc_i = 0.5$.

The numerical solution of the NS equations was accomplished by a completely implicit integrointerpolation technique.[5] The fluxes in semifull nodes were approximated by central second-order differences on a nine-point box scheme. The problem was solved by applying a nonuniform grid with node clustering near a shock wave and a streamlined surface. A modified Newton–Raphson method was employed to solve nonlinear difference equations, and the solution of a linearized set of difference equations was obtained by using LU decomposition with a preliminary permutation of unknowns by the nested dissections method.[6] The numerical computation presented here was performed on an IBM RS 6000/58H computer; one version on a $61 \times 51$ grid required about 30 CPU minutes. The computation technique was tested many times in numerical experiments and proved to be a reliable and highly efficient solution code. For example, Fig. 2 shows the calculation data on temperatures for different degrees of freedom and concentrations of $e$, $NO^+$, $N_2^+$, $O_2^+$ along the stagnation line. The flight altitude was 80 km, velocity was 8.0 km/s, $R \approx 1.2$ m, and the wall was catalytic. When performing a large series of parametric calculations for ionization in a viscous shock layer, parabolized Navier–Stokes (PNS) equations[7] often are used. It was found that maximum levels of $n_{e0,m}$ obtained by use of these models differ little from the results obtained when the NS model is used.[8]

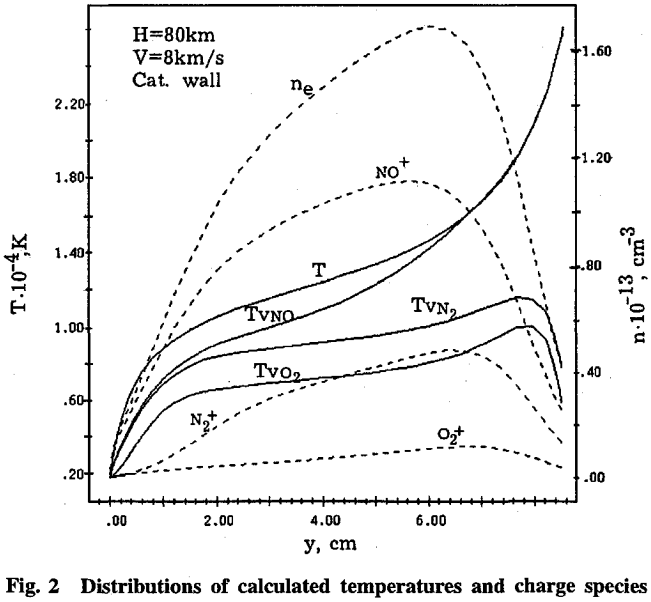


**Fig. 2 Distributions of calculated temperatures and charge species concentrations along the stagnation streamline.**

## Approximate Simulation in Wind Tunnels

The laboratory experiment is the least developed constituent of the complex approach to the investigation of ionization in hypersonic flows. This is attributable to technological and methodological difficulties encountered in simulating nonequilibrium ionization processes in present-day wind tunnels. The simulation of ionization processes in wind tunnels is complicated by two factors. First, the reproduction of real space-time characteristics of ionization and recombination processes in wind tunnels presents certain difficulties. Second, the test-section gas flow in high-enthalpy wind tunnels is, as a rule, a substantially nonequilibrium one in terms of vibrational molecular energy, dissociation, and ionization, and the gas itself can contain various impurities that are difficult to control.

Up-to-date wind tunnels are essentially incapable of simulating nonequilibrium processes completely. Even in high-enthalpy impulse wind tunnels (IWTs), it is impossible to attain altitudes and velocities typical of those during ballistic and gliding re-entry of hypersonic vehicles. The capabilities of present-day IWTs[9] are shown in Fig. 1, curve 6. So, only approximate, partial simulation is implied when discussing the investigation of ionization in wind tunnels.

The simulation of ionization in the case of hypersonic flows over bodies suggests the fulfillment of the similarity laws for a gasdynamic flowfield and kinetic processes. The gasdynamic simulation of hypersonic flows can be performed in up-to-date wind tunnels for particular flight conditions. For example, flows over blunted bodies in regimes featuring the viscosity effects under hypersonic stabilization ($M \geq 10$) are successfully simulated by $Re_0$ in reproducing experimentally the temperature factor and catalytic properties of a streamlined surface. The simulation problem becomes much more complicated when nonequilibrium ionization is considered. The fulfillment of the results of conditions $Re_0 = Re_0^*$, $\Lambda_i = \Lambda_i^*$, $\Lambda_r = \Lambda_r^*$ is an unrealistic requirement for a complete reproduction of flight conditions in wind tunnels. The rule of binary similarity $\rho_\infty R = (\rho_\infty R)^*$ enabling an approximate simulation of nonequilibrium processes in flows over bodies cannot be employed because, so far, it has been impossible to reproduce in wind tunnels the velocity, composition, and thermodynamic state of a gas at flight conditions. Thus, an approximate approach to the simulation of ionization in wind tunnels, based on the application of a combination of the parameters $Re_0$ and $\Lambda_i$, is considered. It is taken into account that in the regimes of a viscous shock layer within the range of values of $V_\infty$, $H$, and $R$ that are of practical interest, the ionization level near a hypersonic vehicle is essentially governed by processes taking place in the regions of flow stagnation, in particular, in the region of nose bluntness. The required combination of $Re_0$ and $\Lambda_i$ is derived from the continuity equation for electron concentration:

$$u\frac{dn_e}{dy} = W_i + \frac{1}{\rho}\cdot\frac{\partial}{\partial y}\left(\frac{\mu}{Sc_i}\frac{\partial n_e}{\partial y}\right) \tag{4}$$

in the form of $\bar{n}_{e0,m} = n_{e0,m}/n_{e0,m}^{eq} \approx f[Re_0\varphi(\Lambda_i)]$ in estimating maximum values of $n_{e0,m}$ along the stagnation streamline. The numerical investigations show that the function

$$\varphi(\Lambda_i) = \int_0^t \frac{W_i dt}{n_{e0}^{eq}}$$

where $W_i$ is the electron formation rate in the shock layer, can be represented with acceptable accuracy by $\varphi(\Lambda_i) \approx \Lambda_i^n/(1+\Lambda_i)^n$, where $n \approx 2$ at $\Lambda_i = 0.01$–1. As shown in Fig. 3, numerous calculations of $n_{e0,m}$ in the viscous shock layer, performed in the United States and Russia, as well as the values of $n_e$ measured in flight tests, correlate well with each other at $Re_0 = 10$–$10^3$, $\Lambda_i = 0.01$–10, and $V_\infty = 4$–8 km/s when they are represented in the form of dependencies $n_{e0,m}/n_{e0}^{eq} = f(K)$, where $K \approx Re_0\Lambda_i^2/(1+\Lambda_i^2)$ or $K \approx Re_0\Lambda_i^2$ at $\Lambda_i \ll 1$. In Fig. 3, the regions of calculated values of $\bar{n}_{e0,m} = f(K)$ are indicated by the hatched band (more details are given elsewhere[10]). Note that at $K \leq 30$, the dependence is divided into two branches, corresponding to catalytic and noncatalytic streamlined surfaces.

Parameter $K$ was used in the approximate simulation of ionization near the vehicle in the viscous shock layer condition performed in a

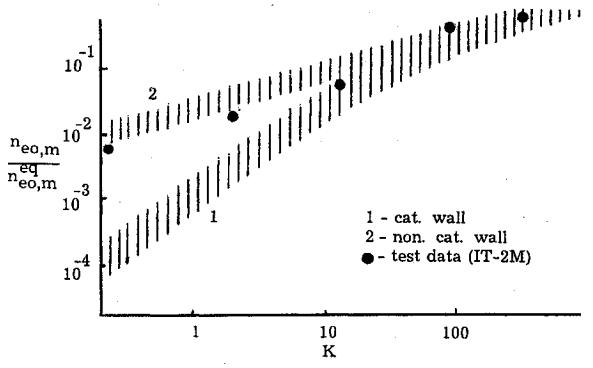


**Fig. 3 Correlation dependence $\bar{n}_{e0,m} = f(K)$.**

hypersonic wind tunnel. It was assumed that the ionization process in the viscous shock layer could be simulated approximately when reproducing in the wind tunnel the correlation parameter $K$ in addition to the main parameters of aerodynamic simulation in the conditions of hypersonic stabilization, i.e., when the condition $K = K^*$ was satisfied. The approximate relation for the simulation condition in the wind tunnel can be derived from the condition $K = K^*$ (at $\Lambda_i < 1$) by using the connection between $\mu_0$, $T_\infty$, and $M$ in the expression $Re_0$:

$$\frac{\rho_\infty R}{\rho^*_\infty R^*} \approx \left(\frac{V_\infty}{V^*_\infty}\right)^{\frac{1}{3}} \left[\frac{\tau_i \rho_\infty}{\tau^*_i \rho^*_\infty}\right]^{\frac{2}{3}} f\left(M/M^*; T_\infty/T^*_\infty\right) \qquad (5)$$

Function $f = (M/M^*)^{0.56}(T_\infty/T^*_\infty)^{0.28} \approx 1$ for the model tests discussed below. At $V_\infty = V^*_\infty$, the same composition and thermodynamic state of a freestream gas under real and tests conditions, Eq. (5) is reduced to the well-known binary similarity law.

Equation (5) allows an approximate consideration of the difference in velocity, composition, and thermodynamic state of flows in wind tunnels and under flight conditions. Along with the multiplier $(V_\infty/V^*_\infty)^{1/3}$, this difference is defined by relation $\tau_i/\tau^*_i$. The characteristic time of ionization behind the shock wave $\tau^*_i$ in wind tunnel conditions depends on the gas composition, on the degree of nonequilibrium in a flow, and stagnation parameters. For the present investigation, the quantity $\tau^*_i$ was determined from the calculated data on ionization in a test gas behind a steady-state shock wave in the test section flow.

## Test Facility

For test investigations, an adequate wind tunnel is of great importance. Emphasis should be placed not only on the possibility of achieving gas flows with high stagnation temperatures $T_0$, but also on the attainment of high pressures $P_{0r}$ in the wind-tunnel reservoir. Increased values of $P_{0r}$ extend the simulation range because of a rise in the binary similarity parameter $\rho_\infty R$ and a decrease in the background electron concentration level in a freestream gas flow. Hypersonic flows with high values of $T_0$ and $P_{0r}$ are comparatively simple to attain in hot-shot-type wind tunnels. Among these is the hypersonic wind tunnel IT-2M of TsAGI. The IT-2M wind tunnel enables a gasdynamic simulation of hypersonic flight conditions over a wide range of Reynolds and Mach numbers. High values of $P_{0r}$ and $T_0$ in this wind tunnel are obtained by impulse ($\tau \approx 0.5$ ms) gas heating in the reservoir (volume 0.9–1.8 dm$^3$) using an electric discharge of 820 kJ. Conical and shaped nozzles to 0.9 m in diameter are used. Hypersonic vehicle models and their components, characteristically 200–300 mm in length, are mounted on stings or suspended by slender stings. The operational parameters of the IT-2M wind tunnel required to investigate ionization are $P_{0r} = 200$–$1000$ atm, $T_0 = 4000$–$8000$ K, $M_\infty = 12$–$21$. Particular attention was paid to the investigations in a high-temperature flow: $T_0 = 7000$–$8000$ K, $P_{0r} = 200$–$300$ atm, $M_\infty = 18$–$21$, $Re_0 = 10^2$–$10^3$. A mixture of nitrogen and a small amount of oxygen (2.5–5.5%) served as the test gas. This mixture represents a tradeoff of the requirements imposed on the simulation of associative ionization process in air against the need to reduce the oxygen content of the test gas to prevent erosion of the discharge chamber walls, electrodes, and the stagnation nozzle section. In the hot-shot wind tunnel the gas flow parameters are continuously varied in the test part of the tunnel. The investigations of ionization processes near the test models were carried out during the first 5–10 ms, when $P_{0r}$ and $T_0$ had high values. At high temperatures, in the IT-2M wind tunnel, copper impurities entering the nozzle and test-section gas flows may be considerable because of discharge-electrode erosion. They have essentially no influence on the aerodynamic and thermal test results, but their role in the ionization process should be elucidated. An analysis showed that, when nitrogen was used as a test gas at $T_0 \leq 4000$ K, the impurity exerted an appeciable effect on the ionization processes in the flow and near the model. However, from comparative analysis of the calculations and tests of ionization in the nozzle and near simple models, it is inferred that the influence of the charged condensate on the ionization kinetics in the IT-2M wind tunnel when the test gas is the mixture $N_2 + O_2$ probably can be neglected at high temperatures, and the associative ionization process of electron formation is the primary effect in the shock layer near the model.

## Diagnostics

Plasma parameters near models in the IT-2M wind tunnel and the flight experiment were measured by use of electric probes. Many publications have been devoted to probe methods, but their applicability in characteristic test conditions, when $M_\infty > 1$, $Kn = 0.1$–$10$ ($Kn$ is the Knudsen number based on the characteristic probe size), has received little attention. Therefore, the operational peculiarities of various probes in supersonic plasma flows were investigated in the electric arc-driven shock tube of TsAGI in an air plasma flow behind the shock wave.[11] Diversified probes, e.g., with cylindrical-shaped electrodes (single, double, triple), conical-shaped (single and double), and with wall electrodes mounted flush with the surface in flow, were investigated. Probes with pointed fairings protecting the electrode surface against liquid or solid particles were designed to measure $n_{e,i}$ concentration in plasma flows containing a condensed-phase impurity. Test data for some probe methods are presented elsewhere.[11]

To find $n_{e,i}$ proceeding from the probe measurements, it is necessary to know the electron temperature $T_e$ in the measurement zone. In some experiments, $T_e$ was estimated from the volt-ampere characteristics of double probes or was measured directly using a triple probe.[11,12] However, in most tests in IT-2M, $T_e$ was obtained using numerical calculations or estimates. This meant that inaccuracy in determining $T_e$ influenced the total accuracy of the probe measurements.

## Numerical Simulation of Ionization Processes in Wind Tunnels

Numerical simulation of nonequilibrium flow in the wind tunnel is based on the solution of equations of gasdynamics and kinetics of nonequilibrium physical–chemical processes taking place in a nitrogen–oxygen mixture at high temperatures. The gas heated in the reservoir at $T_0 \leq 8000$ K is a mixture of the following species: $N_2$, $O_2$, N, O, NO, $N_2^+$, $O_2^+$, $NO^+$, and $e$. Control calculations were carried out with consideration of copper impurities in the gas, the amounts of which were estimated from evaluation of copper-electrode erosion. In the numerical solution, account was taken of the main reactions proceeding in the above-mentioned mixture, nonequilibrium excitation of molecular vibrational degrees of freedom in a multitemperature scheme, as well as ionization that occurs in terms of associative ionization reactions. Influence of the boundary layer on the nozzle walls was taken into account by the iterative method, using the measured values of pressure $P_0$ in the flow at the nozzle exit. Examples of calculations of $T_v$ and $n_e$ in the nozzle in IT-2M are presented elsewhere.[8] The calculation results for the wind-tunnel circuit flow served as initial data to calculate flows over models of simple configurations in the test section. Ionization in the viscous shock layer near models in the IT-2M wind tunnel was determined from PNS[7] calculations. In all, the kinetic model of nonequilibrium processes in the viscous shock layer was similar to that applied to calculate ionization under flight conditions. The parameter $(\rho\tau_i)^*$ is necessary for application of this proposed

method of ionization modeling. To determine this parameter, calculations of ionization time behind the shock wave in nonequilibrium gas flow in the test section of the IT-2M wind tunnel were carried out. The time $\tau_i^*$ was determined from the calculations of the profile of $n_e$ behind a steady-state shock wave in the form

$$\tau_i^* = n_{e,\mathrm{qs}} \Big/ \left(\frac{\mathrm{d}n_e}{\mathrm{d}t}\right)_m$$

where $n_{e,\mathrm{qs}}$ is the quasistationary level of $n_e$ behind the shock wave.

## Applicability of Simulation Principles

First, it is necessary to establish whether the measured values of $n_{e0,m}$ in the IT-2M wind tunnel agree with the correlation dependence $\bar{n}_{e0,m} = f(K)$. The control experiments carried out at $M_\infty = 21$, $T_0 = 7000$ K, $\rho_\infty = 1.5 \times 10^{-7}$ g/cm$^3$ involved measurements of electron concentrations in the vicinity of the stagnation point of a model with the bluntness radius of $R = 0.01$–$0.15$ m, the model surface being noncatalytic. Figure 3 shows the test results. Each test point was obtained by averaging over five runs of the IT-2M wind tunnel. The value of $n_{e0,m}^{\mathrm{eq}}$ measured in the tests was about $10^{13}$ cm$^{-3}$. It is seen that the measured values of $\bar{n}_{e0,m}$ are in agreement with the correlation dependence $\bar{n}_{e0,m} = f(K)$ for ionization near the noncatalytic surface.

In addition to the wind-tunnel simulation in terms of parameter $K$, it is necessary to simulate the hypersonic viscous shock layer condition and the surface boundary conditions, particularly the influence of catalytic surface properties. The capability of the simulating model boundary conditions corresponding to a catalytic surface and a noncatalytic one in a hot-shot-type wind tunnel was verified experimentally. Distributions of $n_e$ across the shock layer were measured near the model featuring cylindrical bluntness, the catalytic surface, which was made of metal, and the noncatalytic surface, which was a dielectric. The results are given in Fig. 4. At a shock-layer thickness of about 5 mm, the distribution of $n_e = f(y)$ ($y$ is the coordinate normal to the model surface on the stagnation line) was measured for $y = 0$–$1$ mm using a double electric probe. These data confirm that the IT-2M wind tunnel is capable of simulating the influence of catalytic properties of a streamlined surface on the distribution of electrons in the viscous shock layer.

The flight altitudes at which the approximate method of simulating ionization is applicable can be derived from relation (5), depending on the quantity $R/R^*$, using the calculated values of $(\tau_i \rho_\infty)^*$. At $V^* = 4.5$ km/s (conditions realized in the IT-2M wind tunnel) and $V = 7.0$ km/s, the applicability of the approximate method of simulating ionization is restricted by the conditions: $H \geq 75$ km at $R/R^* = 5$ and $H \geq 85$ km at $R/R^* = 20$. The calculations performed using the PNS model show that, at these altitudes, the effect of the difference in temperatures, $T_w$ and $T_w^*$, at a streamlined surface on value $N_{e0,m}$ does not exceed about 20%.

Comparison of wind tunnel data with flight test results and numerical investigations serves as a validation process for the approximate simulation concept. Thus, a direct comparison of the computational and wind tunnel test results with the flight tests of Bor-4c was carried out.

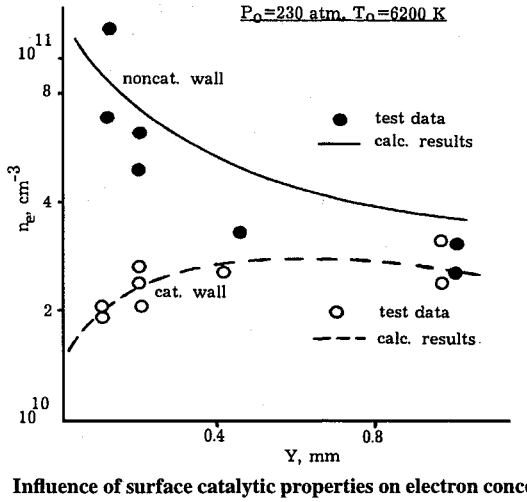


**Fig. 4 Influence of surface catalytic properties on electron concentration in the viscous shock layer.**

## Flight Experiment

The flight experiment is a very important component of the investigation of ionization processes near hypersonic vehicles. The results obtained were used to verify the numerical models of ionization processes and methods of an approximate simulation of ionization in wind tunnels. The flight experiments were carried out on the Russian hypersonic vehicle Bor-4c, designed for aerodynamic and thermophysical investigations under flight conditions. Figure 5 shows the Bor-4c configuration, which is a hypersonic lifting body. Wings with outboard panels and the central fin installed on the afterbody were used for aerodynamic control. The characteristic nose bluntness radius near the stagnation point was about 0.7 m. In a suborbital-flight version, the Bor-4c vehicle was launched to an altitude $H \approx 200$ km by a two-stage rocket; then, it entered the dense atmospheric layers at a velocity of 7.28 km/s. Following aerodynamic deceleration, the vehicle landed using a parachute system.

The plasma parameters in a shock layer were measured at altitudes ranging from 105 to 70 km at flight velocities of $V_\infty = 7.28$–$6.9$ km/s. Measurements were performed with electrostatic probes of two types. Ion concentration inside the shock layer was measured using two double probes placed symmetrically about the vehicle datum line,[8] one probe being 24.5 mm from the vehicle surface, the other at 13.5 mm. Two cylindrical electrodes 1.0 mm in diameter were attached to each probe. The length of the sensitive zone of the electrode probes was 20 mm. The electrodes were made of tungsten and were covered with a chromium coating to avoid oxidation.

The probes were energized by a 12-V sawtooth voltage generator to obtain complete volt-ampere characteristics of each branch of the probe for each second of the flight. The ion density in the wall layer was measured by two double-wall probes that were two electrodes lying in one plane and fixed in a common insulating case. The sensitive probe surface was flush with the heat-resistant coating of the vehicle in an area 0.63 cm$^2$, and constant voltage applied to the probes was $-20$ V. The cylindrical probes retained their normal operating characteristics up to an altitude of $H \approx 70$ km, whereas the wall probes were serviceable up to $H \approx 60$ km. The gas parameters in the shock layer were evaluated relative to the pressure distributions measured on the spherical Bor-4c nose cap and the conjugate windward surface; trajectory parameters and onboard measurements of vehicle motion parameters were recorded as well. Figure 6 shows the flight-test ionization data as a function of flight altitude and flight time. The probe-measured results are shown in Fig. 6 in the form of crosshatched band 1 for the cylindrical probes and band 2 for the wall probes. The "wavy" behavior of measured dependencies $n_e = f(t)$ is attributable to considerable variations in the vehicle angle of attack from 10 to 75 deg in the flight-time interval 490–520 s. At $H = 100$ km, radio communication with ground-based observation posts was lost due to radio blackout and reestablished at $H = 93$ km. The calculated equilibrium value of the electron concentration in the vicinity of the stagnation point is shown in Fig. 6 by line 3. It is seen that, at $H > 80$ km, the ionization processes in the viscous shock layer ($Re_0 < 10^3$) became substantially nonequilibrium. An interesting fact is revealed when comparing the measured value of $n_e$ inside the shock layer with that in the wall region. At $H \geq 85$ km, the value of $n_e$ in the wall plasma layer exceeds that measured at a distance

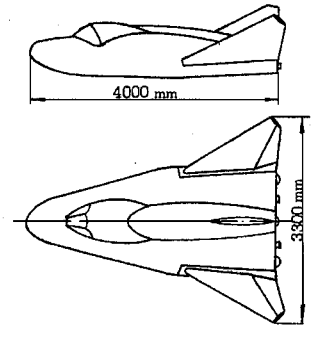


**Fig. 5 Hypersonic vehicle Bor-4c scheme.**

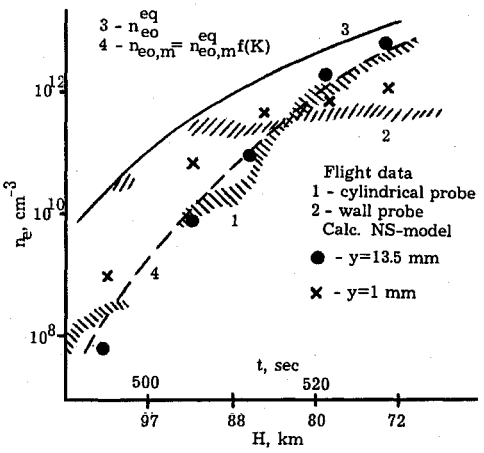


**Fig. 6 Bor-4c flight-test ionization data.**

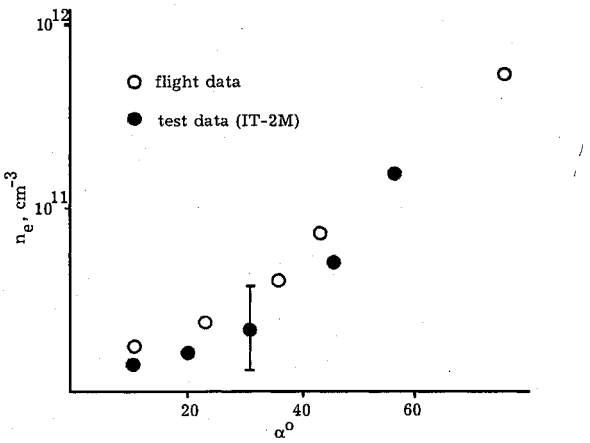


**Fig. 7 Comparison of flight and laboratory data of $n_{e,i}$ near the lower surface of the Bor-4c.**

of 13.5–24 mm. This difference increases as the altitude increases, becoming an order of magnitude and greater at $H > 90$ km. At $H < 80$ km, value of $n_{ew}$ is lower than that of $n_e$ inside the shock layer. Note that, whereas the values of $n_e$ inside the layer vary by almost 3 orders of magnitude in the range $H = 93$–72 km, the measured value of $n_{ew}$ only changes several times, and the effect of the "stabilization" of values of $n_{ew}$ is exhibited in the range $H = 84$–70 km. This effect was caused by measurement of $n_e$ during the flight test near the electrical insulating, noncatalytic heat-resistant coating, its surface temperature not exceeding 700 K at $H \geq 80$ km. The increased gas density near the cold noncatalytic wall when recombination in the wall layer is "frozen" can cause the above-mentioned effect.

## Comparison of Results

Figure 6 shows the calculated values of $n_{ew}$ (line 2) and $n_e$ (line 1) at a distance of 13.5 mm from the surface. The calculation is accomplished by using the numerical NS model. The noncatalytic surface temperature is $T_w = 500$ K, and the gas composition for the flight altitudes is included. As a whole, the ratio between $n_{ew}$ and $n_e$ in the shock layer is confirmed by the calculation. Note that the calculated values of $n_e$ for $y = 13.5$ mm at $H \leq 92$ km are in good agreement with the flight-test results. The discrepancy between the calculation and the test at $H \approx 100$ km can be attributable to the limited applicability of the NS model at $Re_0 \approx 10$. The calculated values of $n_{ew}$ differ from the measured ones to a larger extent, especially at high altitudes. This is attributable to both the simplified form of the boundary conditions used in the calculation and the uncertainty in the physical–chemical processes in a layer with high gradients, and high measurement errors when the plane wall probes are used. Also note that flight-test results (line 1) are in good agreement with the calculation carried out using correlation dependence $\bar{n}_{e0,m} = f(K)$ (curve 4).

The results of flight and laboratory experiments were compared in terms of the ionization parameters near the 1:20-scale Bor-4c

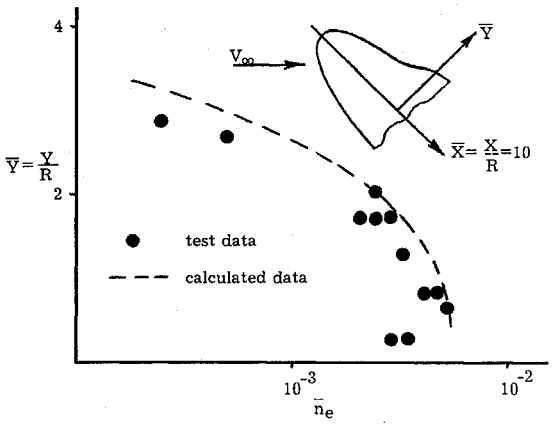


**Fig. 8 Distribution of $\bar{n}_e$ in the plane of symmetry in leeward zone of the Buran hypersonic vehicle.**

vehicle model measured in the IT-2M wind tunnel. Ion and electron concentration was measured on the Bor-4c model in the IT-2M wind tunnel in the probe location zones typical for the flight test. It was possible to reproduce absolute values of $n_{e0}^{eq}$ at $K = K^*$ corresponding to the flight altitude of $H \approx 85$ km. At $H = 87.5$–85 km, the angle of attack varied from 10 to 75 deg. Figure 7 presents some probe measurement results in the shock layer near the lower surface of Bor-4c depending on the angle of attack $\alpha$, and respective measurement data obtained in the IT-2M wind tunnel. A satisfactory agreement of values of $n_e$ measured in flight and test conditions was observed. This finding and comparison of distributions of $\bar{n}_{e,i}$ near various models measured in the IT-2M wind tunnel with the results of other flight tests and model calculations confirm the correctness of the suggested procedure for approximate simulation of ionization processes near a hypersonic vehicle.

Note once again that the simulation of absolute values of $n_e$ near a hypersonic vehicle in the wind-tunnel conditions is possible only for rather limited cases. A simpler problem is the simulation of relative distributions of $\bar{n}_e$ near a hypersonic vehicle only for $K = K^*$.

## Examples of Ionization Investigations

A great deal of data on distributions of $n_{e,i}$ in windward and leeward flow zones near models of various hypersonic vehicles and their components have been obtained by applying the approximate simulation of ionization processes as described in this paper. The plasma parameters were investigated in separation zones, in near-wake regions, near outboard wing panels and control surfaces, and in areas appropriate for radio communication antennas. For example, Fig. 8 shows the distribution of $\bar{n}_e = f(\bar{Y})$ measured in the IT-2M wind tunnel in the plane of symmetry in the leeward zone near the model of the hypersonic vehicle Buran in the section $\bar{X} = 10$ ($\bar{X} = X/R$). In Fig. 8, $\bar{n}_e = n_{e0}/n_{e0}^{eq}$, where $n_{e0}^{eq}$ is the equilibrium electron concentration in the vicinity of the stagnation point. The flight regime at $H = 80$ km was simulated in terms of parameter $K$. The dotted line refers to the inviscid calculated values of $\bar{n}_e$ in the leeward zone near the Buran vehicle. Similar measurements of distributions of $\bar{n}_e$ were made in different planes passing through the vehicle datum line. These data were used to derive the distribution of $\bar{n}_{em} = n_{em}/n_{e0,m}$ ($n_{em}$ is the maximum value of electron concentration in the plasma layer, and $n_{e0,m}$ is the value in the vicinity of the stagnation point) in the cross section $\bar{X} = 10$ as a function of the angle $\varphi$. These results are presented in Fig. 9. The angle $\varphi$ was measured from the plane of symmetry in the leeward zone. From Fig. 9 it is inferred that minimum values of $\bar{n}_{em} \leq 10^{-3}$ are characteristic for the leeward zone at $\varphi = 45$–50 deg. When approaching the plane of symmetry ($\varphi = 0$), the value of $\bar{n}_{em}$ increases several times. Figure 10 presents the distribution of $\bar{n}_e = n_e/n_{e0,m}$ in the plane of symmetry behind the Bor-4c vehicle model. The 1:20-scale model was installed in the IT-2M wind tunnel using a string supension at $\alpha = 45$ deg and $M_\infty = 18$. Similar distributions of $\bar{n}_e$ were evaluated in different sections of the near wake behind the Bor-4c model. Using these data as a base, the approximate three-dimensional distribution of $n_e$ in the vehicle wake

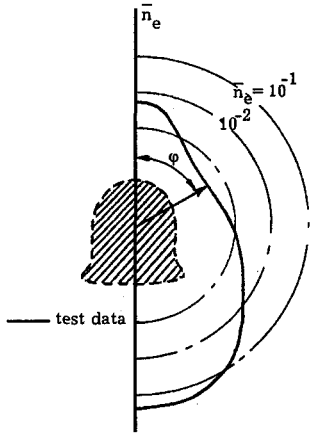


**Fig. 9 Test data distribution of $\bar{n}_e = f(\varphi)$ near the Buran hypersonic vehicle in the cross section $\bar{X} = 10$.**

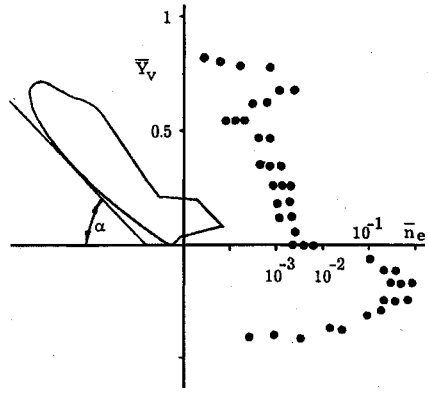


**Fig. 10 Test distribution $\bar{n}_e$ behind Bor-4c.**

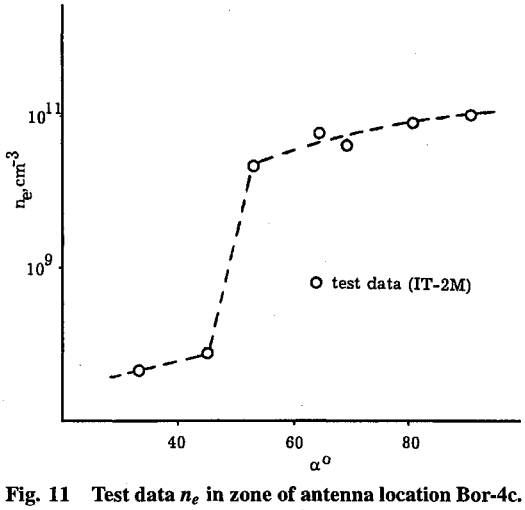


**Fig. 11 Test data $n_e$ in zone of antenna location Bor-4c.**

for the frozen recombination condition was obtained to calculate the propagation of radio waves through the near-wake zone in different directions.[8]

The model tests in the wind tunnel and the simultaneous flight experiment complement each other. For example, in the flight of the Bor-4c vehicle, the communication broke off, as noted, at an altitude of 100 km, and then reestablished at $H = 93$ km. To simulate this situation in the IT-2M wind tunnel, a special experiment was undertaken that implies measurement of $n_e$ concentration on the outboard wing panels in the antenna location area on the Bor-4c vehicle. The tests were made at $T_0 = 7000$ K in the viscous shock layer. Figure 11 shows the behavior of $n_e$, depending on the angle of attack in this zone. It is seen that changes in the flow at $\alpha = 40$–60 deg result in a strong increase in $n_e$ (by more than two orders of magnitude) on the outboard wing surface. This effect probably is responsible for the breaking off of communications at $H = 100$ km when the angle of attack rises up to 60 deg in the flight of the Bor-4c vehicle and its reestablishment at $H = 93$ km when the angle of attack decreases to 20 deg.

During the investigations of ionization in the IT-2M wind tunnel, the effects of different parameters on ionization processes in hypersonic flows over bodies were evaluated. In particular, the influence of distributed cold gas injection on ionization in a viscous shock layer and the formation of a separated flow zone in the region of bluntness were investigated.[8]

## Conclusion

Having read the present article, one may ask why complicated wind tunnel and flight experiments should be carried out and a very approximate approach to the laboratory simulation of nonequilibrium ionization processes be employed if the current state of the art in computational fluid dynamics allows the computation of three-dimensional distributions of the electron concentration and other parameters of plasma near a hypersonic vehicle. Two answers may be given.

First, wind-tunnel tests were indispensable, because at the time that they were conducted, adequate computing facilities were not available to solve viscous three-dimensional problems including nonequilibrium physical–chemical processes based on the Navier–Stokes equations.

Second, we believe that, even with the availability of modern high-efficiency computers, a diversity of problems can be solved in a more rational way on the basis of laboratory experiments. Among these are the investigation of different processes (fluid injection into the viscous shock layer, action of electric and magnetic fields), and the analysis of various methods providing the transformation of kinetic energy of plasma to electric energy.

## Acknowledgments

The investigation was supported by Grant 94-01-01381 of the Russian Fund of Fundamental Investigations. The authors thank B. M. Fedosov, V. S. Nikol'sky, L. A. Kildushova, and V. G. Tchebureev for their participation in this work.

## References

[1]Park, C., "Review of Chemical-Kinetic Problems of Future NASA Mission, I: Earth Entries," *Journal of Thermophysics and Heat Transfer*, Vol. 7, No. 3, 1993, pp. 385–398.

[2]Kang, S. W., Jones, W. L., and Dunn, M. G., "Theoretical and Measured Electron-Density Distributions at High Altitudes," *AIAA Journal*, Vol. 11, No. 2, 1973, pp. 141–149.

[3]Losev, S. A., Makarov, V. N., Pogosbek'yan, M. Y., Shatalov, O. P., and Nikol'sky, V. S., "Thermochemical Nonequilibrium Kinetic Model in Strong Shock Waves in Air," AIAA Paper 94-1990, June 1994.

[4]Beeryukov, A. V., "Kinetic of Physical Process in Gasdynamics Lasers," *Proceedings of the Physical Institute of Academy of Science USSR*, Vol. 83, 1975, pp. 13–86.

[5]Yegorov, I. V., and Zaitsev, O. L., "Development of Efficient Algorithms for Computational Fluid Dynamic Problems," *Proceedings of the 5th International Symposium on Computational Fluid Dynamics*, Sendai, Japan, Vol. 3, 1993, pp. 393–400.

[6]George, A., "Nested Dissection of a Regular Finite Element Mesh," *SIAM Journal of Numerical Analysis*, Vol. 10, No. 2, 1973, pp. 347–363.

[7]Cheng, H. K., "Perspective on Hypersonic Viscous Flow Research," *Annual Review of Fluid Mechanics*, Vol. 25, 1993, pp. 455–484.

[8]Gorelov, V. A., Gladyshev, M. K., Kireev, A. Y., Korolev, A. S., Nikol'sky, V. S., Byzov, V. N., and Fedosov, B. M., "Ionization Near Hypersonic Vehicles: The Experience of Numerical, Laboratory and Flight Investigations," AIAA Paper 95-1940, June 1995.

[9]Laster, M. L., and Bushell, D. M., "A National Study for Hypersonic Facility Development," AIAA Paper 94-2473, June 1994.

[10]Gorelov, V. A., Nikol'sky, V. S., and Korolev, A. S., "About Ionization in Viscous Shock Layer and This Process Simulation in Laboratory Experiment," *Applied Mathematics and Technical Physics*, No. 6, 1985, pp. 121–127 (in Russian).

[11]Gorelov, V. A., Kildushova, L. A., and Kireev, A. Y., "Ionization Particularities Behind Intensive Shock Waves in Air at Velocities of 8–15 km/s," AIAA Paper 94-2051, June 1994.

[12]Chen, S. L., and Sekiguchi, T., "Instantaneous Direct-Display System of Plasma Parameters by Mean of Triple Probe," *Journal of Applied Physics*, Vol. 36, No. 8, 1965, pp. 2363–2375.

K. J. Weilmuenster
*Associate Editor*